

## Finite element modelling of reheat cracking initiation in austenitic weldments

R A W BRADFORD BA, PhD, MInstP  
Nuclear Electric Limited, Barnwood, UK

### SYNOPSIS

A quantitative model of the initiation of reheat cracking in austenitic stainless steel weldments is presented and applied to a wide range of plant geometries. The key feature of the model which permits the prediction of reheat cracking is the sensitivity of the creep ductility to the state of triaxial stress (constraint).

### 1. INTRODUCTION

Reheat cracking is the phenomenon whereby cracks occur during exposure to creep regime temperatures, predominantly due to the relaxation of welding residual stresses. Consequently, reheat cracks can form during service in non-stress-relieved weldments if creep temperatures prevail. Reheat cracking in austenitic material was first observed in Nuclear Electric plant in 1988, and has since been found in five of British Energy's seven AGR Power Stations. Companion papers in these proceedings summarise the strategy which has been adopted within Nuclear Electric in order to ensure safe reactor operation despite the reheat cracking phenomenon. One aspect of this strategy has been a large programme of work to further understanding of the reheat cracking mechanism. This paper summarises the structural analysis work completed to date as part of this programme.

### 2. CREEP DAMAGE LEADING TO REHEAT CRACKING

The model which has been developed within Nuclear Electric presumes reheat cracking to be initiated when the creep strain ( $\epsilon_c$ ) accumulated at a point reaches the local creep ductility at that point ( $\epsilon_p$ ). These strain measures are equivalent Mises strains, the models being based on standard isotropic Mises flow theory. The model employs a creep ductility which is dependent on the stress state (see Section 3). The ductility is also strain rate dependent (see Section 6). Consequently, the ductility varies from point to point because the stress state and

the strain rates will differ at different points. Similarly, the ductility at a point changes over time because the stress state and the strain rates will also change over time. A convenient measure of the creep damage accumulated at a point is therefore defined by,

$$D_c = \int_0^t dt \frac{\dot{\epsilon}_c}{\epsilon_f} \quad (1)$$

where  $\dot{\epsilon}_c$  is the creep strain rate. Initiation of cracking is predicted when, and where,  $D_c$  first reaches unity. This formulation of creep damage, essentially a simple continuum damage mechanics approach, has been implemented within the general purpose finite element program ABAQUS via a User subroutine which evaluates the above damage integral numerically.

This model is, strictly, limited to the initiation of reheat cracking. Nevertheless, conclusions regarding the depth and orientation of potential reheat cracks can be drawn from the zones of damage and the extent of the tensile welding residual stresses.

### 3. EFFECTS OF MULTIAXIAL STRESS STATE

The model assumes that the effect of a triaxial stress state is to modify the creep ductility according to the following equation,

$$\epsilon_f = \epsilon_{f,uni} \exp \left[ p \left( 1 - \frac{\sigma_1}{\bar{\sigma}} \right) \right] \cdot \exp \left[ q \left( \frac{1}{2} - \frac{3\sigma_p}{2\bar{\sigma}} \right) \right] = S \epsilon_{f,uni} \quad (2)$$

where  $\epsilon_{f,uni}$  is the uniaxial creep ductility,  $\epsilon_f$  is the multiaxial creep ductility,  $\sigma_1$  is the maximum principal stress,  $\sigma_p$  is the hydrostatic stress, and  $\bar{\sigma}$  is the Mises equivalent stress ( $S = \epsilon_f / \epsilon_{f,uni}$  will be referred to as the ductility ratio). The parameters  $p$  and  $q$  have been determined empirically for the class of materials of interest (316H stainless steel) as  $p = 2.38$  and  $q = 1.04$ . These values have been shown by laboratory tests to be appropriate under conditions of triaxiality and strain rate comparable to that of plant situations.

### 4. THE FINITE ELEMENT MODELS

The reheat cracking initiation models include the following steps; (i) modelling the welding residual stresses, (ii) modelling a pre-service overpressure test, where relevant, (iii) raising to operating temperature, (iv) applying service loadings, eg. pressure, thermal stresses, system stresses etc, (v) modelling creep effects during service life. Steps (i) to (iv) are elastic-plastic analyses, whereas step (v) is an elastic-creep analysis. Inclusion of work hardening up to 10% strain in the parent material is important in order to model correctly the initial residual stress magnitudes.

The most time consuming part is to determine the residual stress field. The requirements of the reheat cracking initiation models are particularly demanding in this respect since the

details of the residual stress variation through the section thickness are important. In addition, all components of residual stress are needed in order to represent correctly the state of stress triaxiality which is crucial to the initiation model (see Section 3).

## 5. VALIDATION OF RESIDUAL STRESS DISTRIBUTIONS

The difficulty of modelling welding residual stresses, together with the importance for the subsequent reheat cracking modelling of doing so accurately, motivates careful experimental validation of the finite element residual stress predictions. This has been done using four different experimental techniques: (a) strain gauge rosettes and centre-hole drilling, (b) deep hole drilling and concentric trepanning, (c) neutron diffraction, and (d) the "Block Removal, Splitting and Layering" (BRS�) technique. The last three techniques all produce profiles of residual stress variation through the section thickness. These techniques have been employed on four different ex-service or mock-up plant geometries; two cylindrical butt welds (one thick, 64mm, and one thinner, 16mm), a thick header-branch geometry, and a highly constrained plate-to-plate T-butt weld. In all cases good agreement between the measured and predicted residual stresses has been found.

## 6. MATERIALS CREEP DATA

The material considered is 316H stainless steel. Relevant creep data assumed are;

Creep Deformation: At low levels of damage, the creep strain rate is given by the RCC-MR code. This is a 'best estimate' of creep strain rates, and has been shown to be representative of Nuclear Electric ex-service 316H material. More generally, at higher levels of damage, the RCC-MR creep strain rates are increased by a factor of  $1/(1-D_c)^3$ . This is to account for tertiary creep effects (the RCC-MR law relates to primary and secondary creep only).

Uniaxial Creep Ductility ( $\epsilon_{t,un}$ ): The uniaxial creep ductility assumed is a lower bound, strain rate dependent formulation derived from tests on ex-service 316H material. This material is known to be susceptible to reheat cracking. In particular, the lower bound, lower shelf creep ductility is 0.9%, this applying at strain rates slower than  $10^{-3}$ /hour. At a strain rate of  $10^{-3}$ /hour the lower bound creep ductility is 3.2%.

## 7. PLANT GEOMETRIES AND LOADING MODELLED

Some 22 different plant geometries have been analysed so far in the programme, including both residual stress modelling and subsequent reheat crack initiation modelling. These include cylindrical butt welds with thicknesses from 13mm to 64mm and R/t ratios from 3 to 25. Also included are a diverse range of non-butt welds, eg. a header-branch geometry, plate/plate T-butt welds, fabricated box-section beams, thin tube to thick casting welds, and other unique feature welds. In some cases weld caps are modelled as dressed smooth and flush, in other cases weld cap and toe features are present. Some geometries include obvious stress raising features near the weldment, others do not. In a few cases, repair welding has also been modelled. As regards loading, in typical cases the service loading is minor compared with the residual stress. However, some analyses do include large service stresses

with a substantial primary component. Hence a very wide range of geometries and conditions has been represented by the whole programme of work.

## 8. EXAMPLE DAMAGE RESULTS AND PLANT EXPERIENCE

As an example, the creep damage map resulting after 8,000 hours and at the end of service life (250,000 hours) is shown in Figure 1 for a header-branch geometry. The earlier time is when the maximum damage first reaches unity, and hence the (subsurface) initiation of cracking is predicted. The maximum depth of cracking during service is illustrated by the damage map at the end of life. This prediction of cracking is born out by plant experience, most of this population of welds having been found to contain reheat cracks in the past. (Most of the defective headers have now been replaced with solution treated branch welds). Consistency between the model and plant observations may be noted in regard to, (i) prediction of cracking at the observed location of cracking, ie. within the header parent material under the weld toe, (ii) no cracking predicted at other positions (and none observed), (iii) predicted time of initiation consistent with time of observed cracking, (iv) prediction of cracking in the observed orientation (based on the assumption that a crack grows perpendicular to the maximum in-plane principal stress), (v) predicted size of damage/tensile zones consistent with the depths of typical observed reheat cracks, (vi) defects are observed to initiate subsurface, consistent with a mechanism dependent on triaxial stressing.

## 9. SUMMARY OF REHEAT CRACKING INITIATION MODEL RESULTS

The intention of this Section is to provide an overview of the key results of all the models of reheat crack initiation completed to date. In particular to elucidate what factors lead to the prediction of, or the absence of, reheat cracking.

### 9.1 Relation of Damage to Minimum Ductility Ratio ( $S_{min}$ )

The constraint of a given geometry, and hence the level of triaxial stressing which arises, is a principal cause of reheat cracking due to its reduction of the creep ductility. The most convenient measure of triaxiality is the minimum ductility ratio,  $S_{min}$  [see Equ.(2), Section 3]. Figure 2 plots end-of-life damage ( $D^{end}$ ) against minimum ductility ratio for all the analyses (different letters represent different geometries). Whilst cracking is not predicted for ductility ratios greater than 0.31, the occurrence of smaller ductility ratios does not necessarily imply that cracking will occur. Hence there is no unique relationship between damage and ductility ratio. Nevertheless, the lines drawn 'by eye' on Figure 2, which bound the data above and below, do indicate a correlation between increasing ductility ratio and decreasing damage (as would be expected).

### 9.2 Relation of Damage to 'Radial' Stress

Another measure of the degree of triaxiality is the magnitude of the smallest principal stress. This is an appropriate parameter because the two larger principal stresses will tend to be large, ie. approaching 'yield' magnitude, because of the non-stress-relieved residual stresses. Hence the discriminator between low and high levels of triaxiality is the magnitude of the

smallest principal stress. Figure 3 plots the end of life damage for all the analyses against the smallest principal stress. An immediate 'rule of thumb' which follows from Figure 3 is that reheat cracking occurs only if the smallest principal stress exceeds 60 MPa, and occurs in all instances where the smallest principal stress exceeds 75 MPa. There is only one exception to this rule, for a weld where the occurrence of cracking is associated with a very high follow-up factor due to large primary service stresses.

### 9.3 Relation of Damage to Follow-Up Factor (Z)

A follow-up factor can be defined as  $Z = E\epsilon_c/\Delta\sigma$ , where E is Young's modulus at the operating temperature,  $\epsilon_c$  is the equivalent creep strain and  $\Delta\sigma$  is the decrease in the Mises stress. The creep strain relates to the totality of loading (residual stresses plus all service stresses), hence the follow-up factors quoted here reflect the nature of this combined loading. If service stressing contains a large primary component, the follow-up factors as defined here will be large. Figure 4 plots end of life damage versus the follow-up factor for all analyses. This Figure suggests that reheat cracking can occur at virtually any level of follow-up (although the smallest follow-up factor for which any of the geometries analysed was found to crack was about 2.0). This is not surprising since reheat cracking has been observed both in cases where service stressing is slight and in cases where service stressing is likely to have played a significant role in the cracking. In the latter cases, the large follow-up factors are a combined consequence of the substantial service stressing together with the presence of stress concentrating features in the geometry. Perhaps most significantly, Figure 4 suggests that reheat cracking is to be expected (for the lower bound 316H creep ductility employed here) if the follow-up factor exceeds about 4.0.

### 9.4 Relation of Damage to the 'Reheat Cracking Parameter' ( $P = Z / S_{\min}$ )

A 'reheat cracking parameter' may be defined as  $P = Z / S_{\min}$ . The motivation for considering this parameter is as follows; ignoring the variation in creep ductility with time, and hence the need to integrate, the damage, defined by Equ(1), reduces to,

$$\begin{aligned} D &= \epsilon_c / \epsilon_r \\ &= Z \Delta\sigma / E S_{\min} \epsilon_{r,\min} \end{aligned}$$

Hence, the maximum damage is,

$$D_{\max} = P \Delta\sigma / E \epsilon_{r,\min}$$

The utility of the reheat cracking parameter (P) is that it might be expected to contain the bulk of the geometry and load dependence of the damage. This is because  $\Delta\sigma / E \epsilon_{r,\min}$  is expected to be of a similar magnitude for all analyses.

Figure 5 plots the end of life damage versus the reheat cracking parameter for all the analyses. As expected, the damage correlates well with this parameter. Figure 5 suggests that, for cracking to occur, the reheat cracking parameter must be about 10.5 or greater. Figure 5 also suggests that reheat cracking becomes probable for  $P > 17$ , although this only applies for materials conforming to the lower bound ductility assumption employed here. A

material with good creep ductility is unlikely to exhibit reheat cracking. For example, a uniaxial ductility of 10% would require  $P$  to be greater than about 100 to cause cracking.

### 9.5 Depth of Damage Zone

Figure 6 plots the end of life depth of the damage zone,  $d^{eol}$ , (ie. the region where the damage reaches unity) against the depth of the tensile residual stress zone. The tensile zone has been defined in two alternative ways; as the depth of the region in which the in-plane (opening mode) stress is tensile ( $d_1$ ), and as the depth over which all three principal stresses are tensile ( $d_2 \leq d_1$ ). For all the analyses carried out,  $d_2$  provides an upper bound to  $d^{eol}$  (and hence  $d_1$  provides a greater upper bound).

## 10. VALIDATION OF THE REHEAT CRACKING INITIATION MODEL

The acid test of the initiation model is its performance when compared with plant experience regarding the occurrence, or absence, of reheat cracking. Of the plant geometries analysed to date, inspection evidence is available for eight populations of weldments. The initiation model generally performs well when compared with the plant evidence regarding the occurrence, location and orientation of reheat cracking. In addition, the initiation model has been validated against laboratory tests which produced cracking from repeated relaxations in notched specimens. It is worth noting that the measured strain to cracking in these tests can be as little as 0.2%, ie. an order of magnitude less than the uniaxial ductility, confirming directly the marked effect of multiaxial stressing on the local creep ductility which is the central feature of the reheat cracking model presented here.

## 11. CONCLUSION

A quantitative model of the initiation of reheat cracking in austenitic stainless steels has been presented, together with a summary of its application to a wide range of plant geometries and loading conditions. Reheat cracking occurs due to a combination of,

- i. non-stress-relieved welding residual stresses,
- ii. low uniaxial creep ductility, especially at low strain rates,
- iii. small triaxial/uniaxial ductility ratios,
- iv. significant stress triaxiality,
- v. follow-up effects.

For a given material, the propensity of a given weld geometry to reheat crack may be measured by a 'reheat cracking parameter' defined as  $P = Z/S_{min}$ , where  $Z$  is the follow-up factor, and  $S_{min}$  is the minimum ductility ratio, given in terms of the triaxial stresses by an equation like Equ.(2).

Encouraging agreement between the model predictions and plant and laboratory incidents of cracking has been found.

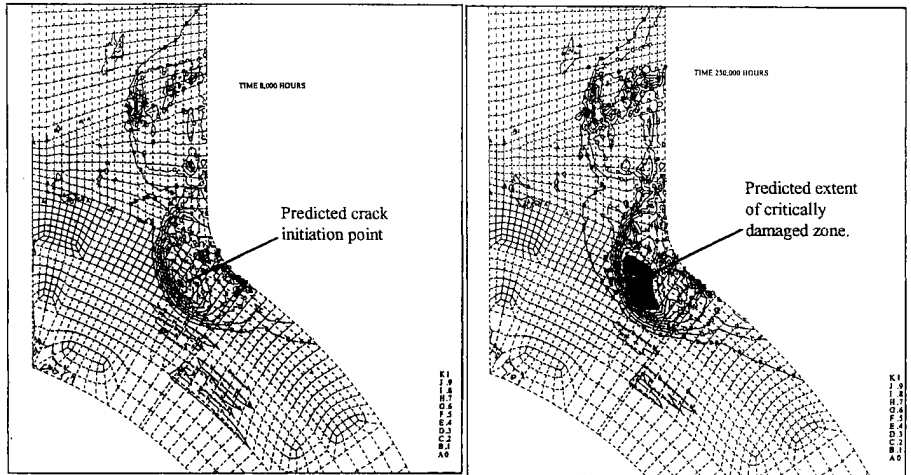


Figure 1: Example of Damage Maps for a Header/Branch Geometry

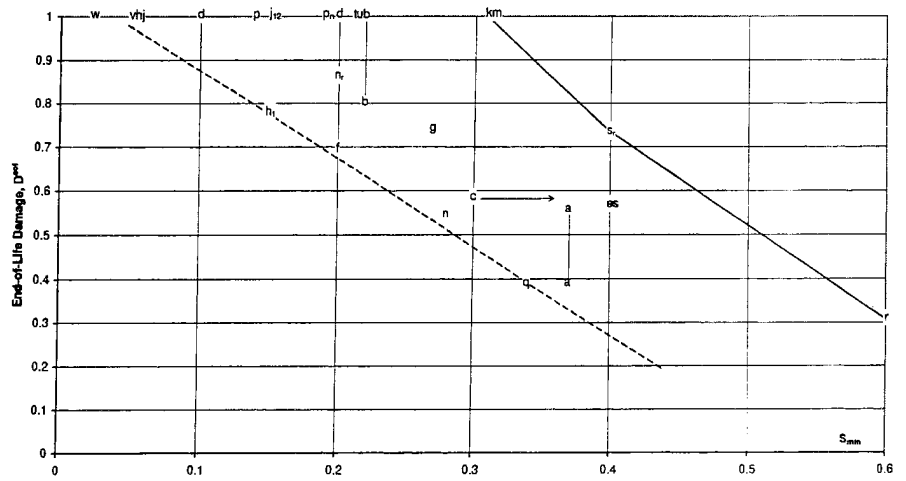


Figure 2: Damage versus Minimum Ductility Ratio ( $S_{min}$ ) for All Models

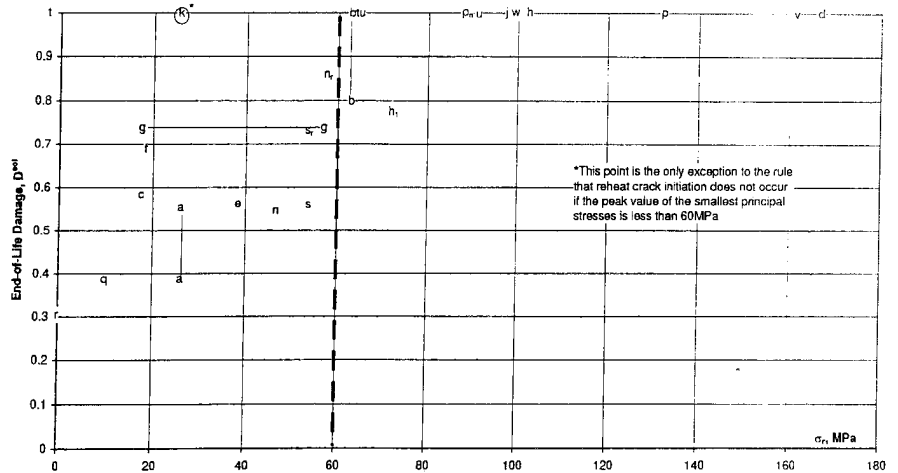


Figure 3: Damage versus Peak Value of Smallest Principal Stress for All Models

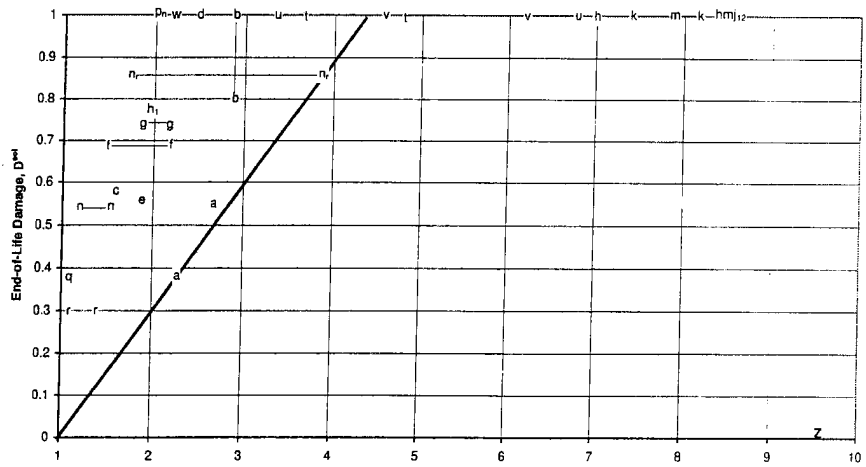


Figure 4: Damage versus Follow-Up Factor (Z) for All Models



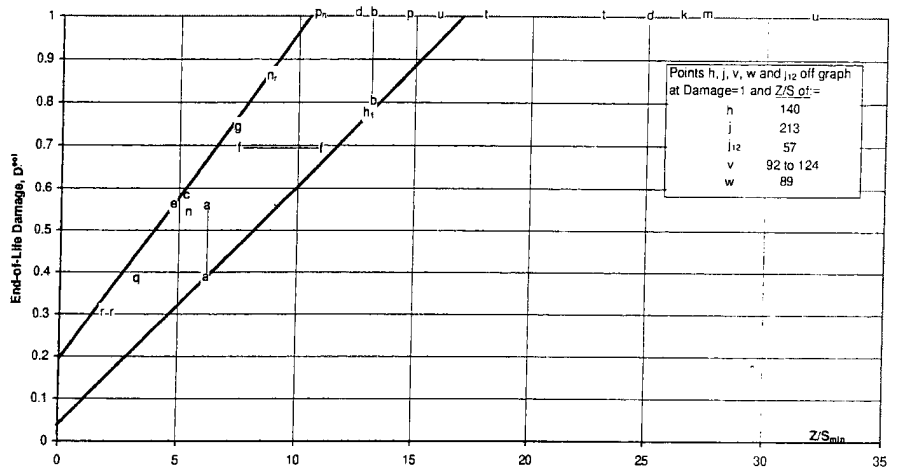


Figure 5: Damage versus Reheat Cracking Parameter,  $Z/S_{min}$

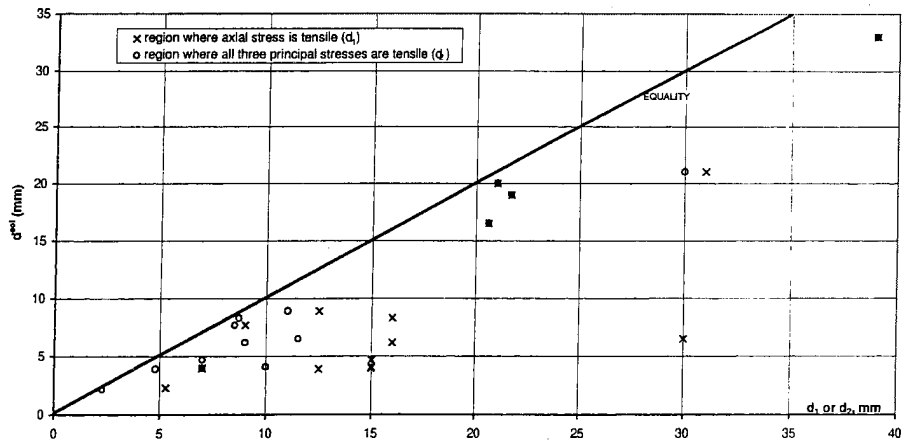


Figure 6: Damage Zone Depth ( $d^{eol}$ ) versus Depth of Region where Start-of-Life Stress is Tensile